Modeling of Isomeric Structure of Diphenyl Urethane by FT-IR Spectroscopy During Synthesis from Phenylisocyanate and Phenol as an Inverse Kinetic Problem

ARTICLE *in* THE JOURNAL OF PHYSICAL CHEMISTRY A · JUNE 2011

Impact Factor: 2.69 · DOI: 10.1021/jp202227d · Source: PubMed

3 AUTHORS:

Nicolas Spegazzini
Massachusetts Institute of Technology
23 PUBLICATIONS **99** CITATIONS
SEE PROFILE

Heinz W Siesler
University of Duisburg-Essen
233 PUBLICATIONS **3,451** CITATIONS
SEE PROFILE

Yukihiro Ozaki
Kwansei Gakuin University
916 PUBLICATIONS **17,663** CITATIONS
SEE PROFILE

THE JOURNAL OF PHYSICAL CHEMISTRY A

ARTICLE

pubs.acs.org/JPCA

Modeling of Isomeric Structure of Diphenyl Urethane by FT-IR Spectroscopy During Synthesis from Phenylisocyanate and Phenol as an Inverse Kinetic Problem

Nicolas Spegazzini,*[,†] Heinz W. Siesler,[‡] and Yukihiro Ozaki[†]

[†]Department of Chemistry, School of Science and Technology, Kwansei Gakuin University, Gakuen 2-1, Sanda, Hyogo 669-1337, Japan

[‡]Department of Physical Chemistry, University of Duisburg-Essen, D 45117 Essen, Germany

ABSTRACT: Isomeric structure of diphenyl urethane during synthesis from phenylisocyanate and phenol has been investigated by modeling the reaction extent as an inverse kinetic problem, using FT-IR difference spectroscopy, to obtain structural information on the formation of the isomeric structure. The aim of this study was to determine the primary algebraic structures (an inverse problem), which describe the chemical reaction system in terms of spectroscopic observables. Moreover, a conventional description of the evolution of chemical species and of the change of moles of the observable species, as a function of time, was explored, defined in terms of the extent of reaction ξ and the reaction stoichiometries ν, based on the Jouguet−de Donder equation, for an invariant system in batch experiments. Two processes for diphenyl urethane with hydrogen bonding and their free form were identified. Experimental input for the identification is a matrix of in situ spectroscopic data A (FT-IR/ATR spectra measured during the reaction process) and a matrix of initial moles (N^0). Subsequently, (1) the number of observable reactions present, (2) the change of moles and their extent of reactions ξ, (3) the reaction stoichiometries ν, (4) the concentration of all observable species (C), and finally (5) the kinetic rate constants were determined. Meaningful extraction of such algebraic system information (an inverse algebraic problem) is a mandatory prerequisite for the subsequent detailed kinetic modeling (an inverse kinetic problem). This research opens up the possibility of modeling the extent of the reaction and performing a kinetic analysis of the hydrogen bonding in an organic system. Important information could be extracted, for understanding of different functions and interactions of hydrogen bonding in a supramolecular system.

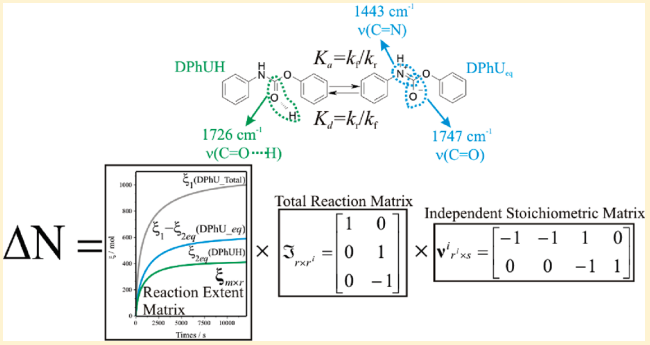

INTRODUCTION

Significant progress in the study of chemical reaction systems is highly dependent on the meaningful extraction of chemical knowledge from large amounts of experimental data. Such experimental measurements can be obtained from a variety of techniques; however, the vibrational spectroscopies (Raman, IR, NIR) are specifically potential tools for this propose.[1] However, systematic and general methodology for the effective analysis and interpretation of complex-mixture spectroscopic data to gain physically and chemically meaningful insight into reactive systems is still limited.[2] Although the above system identification methods are useful for any arbitrary reaction system,[3] the above issues are particularly relevant to the most general and widespread problem in the chemical sciences, system identification in chemical reaction modeling.[4−8] Typically, such liquid-phase reactive systems are initiated by introducing various amounts of reactants into a liquid-phase batch reactor. When in situ observations of such systems are performed, one or more online spectrometers may be used. The spectral time series obtained during the reaction contains information about the time-dependent concentrations of reactants, intermediates, and products.[9,10]

For obtaining real-time information about chemical composition, IR spectroscopy has proved to be highly versatile, especially when performed with the attenuated total reflection (ATR) technique. ATR probes allow the acquisition of precise information about chemical components with short optical path lengths (0.5−3 μm), and the fiber cables provide the flexibility for adapting the devices to new systems, leading to reproducible results as compared to metallic lightguides.[11−13] Time-resolved FT-IR spectroscopy is one of the most popular used spectroscopic techniques for characterization and for monitoring in situ reactions.[14−18] FT-IR difference spectra obtained by this technique enhance the spectroscopic changes occurring during the chemical process, for example, photochemical processes.[19,20] Classical kinetic analysis based on a study of single channel (wavenumber or wavelength) traces has a limited performance to deal with chemical reaction processes due to the spectroscopic overlap of coexisting evolving species and to the impossibility to

Received: March 9, 2011
Revised: June 25, 2011
Published: June 27, 2011

Scheme 1. Reaction of Diphenyl Urethane from Phenol and Phenyl Isocyanate and the Isomeric Structures of Diphenyl Urethane

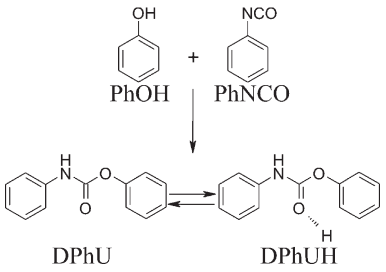

detect interfering species in the measured signal. For this reason, chemical reaction modeling is needed to improve the extraction of chemical information.

As a starting point of view, the application of physical and chemical theories allows us to make predictions: given a complete description of a chemical system, we can predict the results of measurements. This problem is called the *modelization* problem, the *simulation* problem, or the *forward* problem.[21−23] It is more difficult to obtain information of a chemical reaction model from a finite number of observations (spectroscopic data). The knowledge of parameters (number of species and reactions, concentration and kinetics constants) of an unknown component then can be indirectly inferred from the experimental observation of the system. Such parameter identification problems belong to the class of inverse problems. In general terms, one looks for the causes of the observed effects. A chemical reaction model problem can be seen as an inverse problem.[21−23] Based on the Jacques Hadamard suggestion[24] about *well-posed* problems, a chemical reaction model problem is often called an *ill-posed* problem, in the sense that there can be multiple solutions that are consistent with the experimental data.[2,25−27] The inverse problems are typically inherently unstable (highly sensitive to data errors). For this reason, one needs to make any available *a priori* information explicit on the model parameters, to solve an *ill-posed* problem. This process is known as regularization.[21,22,28−30]

Using the concept of the inverse problem for a chemical reaction model parameters will be derived from spectroscopic data. Using this approach, a description of chemical transformation from the extent of reaction (ξ) to the reaction advancement ratio (χ) is possible. Finally, the kinetic parameters are identified. The principal aim of this Article is to determine the kinetics and the mechanism for the formation of the isomeric structures and to quantify these structures (Scheme 1). This methodology is used here: the inverse reaction extent of an eigenvalue problem[31] is regularized to identify the parameters of the chemical reaction, as follows:

(1) Determine the number of observable reactions, change of moles, extent of reaction, reaction stoichiometries, and the concentration of any species in the system.
(2) Determine the kinetic constants considering a nonlinear least-squares minimization problem; using the information minimized for the reaction extent model and simulation based on ordinary differential equation (ODE).

In previous studies, the synthesis of diphenyl urethane by the reaction of phenol with phenylisocyanate has been monitored, thereby demonstrating the applicability of remote analysis over a distance of 90 m between the spectrometer and the measuring position by near-infrared spectroscopy.[32] Fiber-optic coupled FT-IR/ATR spectroscopy has also been applied to study the same reaction.[33] It was shown that the evolution of a ν(C═O) band doublet due to free and hydrogen-bonded carbonyl groups of the diphenyl urethane product was explained by the possible presence of two isomeric structures (Scheme 1) where one of them forms hydrogen bonds with itself or with the OH group of the reactant phenol.

In the present study, the isomeric structure of diphenyl urethane is analyzed during the synthesis from phenylisocyanate and phenol at different temperatures.

THEORETICAL BACKGROUND

Description of the Chemical Reaction: From the Extent of the Reaction Model ξ to the Reaction Advancement Ratio χ. In general, all component reactants (R) and products (P) of a reaction system with m elements can be expressed by a linear combination of e elements, as a balanced mass. The b denotes the number of moles of reactants or products that participates in the reaction, eq 1.

$$\mathbf{M} = \sum_{k=1}^{e} b_{ik} \cdot R_k = \sum_{k=1}^{e} b_{ik} \cdot P_k \quad (i = 1, 2, \ldots, \ldots m) \tag{1}$$

where $\mathbf{M}$ is the chemical reaction matrix.

The stoichiometric equation would be the following eq 2:

$$0 = \sum_{i}^{m} \nu_i \mathbf{m}_i = \nu \cdot \mathbf{M} \tag{2}$$

with $\mathbf{m}$ being is the chemical reaction vector, and ν_i (stoichiometric coefficient) > 0 for the products and <0 for the reactants. At the initial time t_0, the system is made up of n_{i0} moles of m components. If the mixture occurs in any proportion, then the limiting reactant (n_{L0}) is called $\mathbf{m}_L$. In this terminology, the lowest value of $n_{i0}/|\nu_i|$ is the starting extent, and $\alpha_L = n_{L0}/|\nu_i|$, where $\alpha_L > 0$, is the limiting extent (both fractional quantities expressed in moles).

The conventional description of the evolution of chemical species can be seen as the change of moles of observable species, in a time interval $t_0 \rightarrow t_n$, $dn_i = \nu_i\, d\xi$, defined in terms of the extent of reaction ξ and the reaction stoichiometries ν. Equation 3 in matrix algebra form provides the representation of the Jouguet−de Donder equation[34] in the case of the represented (invariant system) semibatch experiments.

$$\Delta \mathbf{N} = \mathbf{N} - \mathbf{N}^0 = \boldsymbol{\xi} \cdot \boldsymbol{\nu} \tag{3}$$

where N^0 represents the initial number of moles.

The reaction advancement ratio $\chi(t)$ is introduced by using the limiting reactant as a reference.[35] Thus, the reactant has completely disappeared, when the reaction is completed, $n_L = 0$.

We can therefore write $\xi_{max} = n_{L0}/|\nu_i| = |\alpha_L$, where $\chi(t)$ is the reaction advancement ratio at the time t. It is a dimensionless number extreme eq 4:

$$\boldsymbol{\chi} = \frac{\mathbf{N} - \mathbf{N}^0}{\boldsymbol{\nu}} \frac{1}{\boldsymbol{\xi}_{max}} = \frac{\boldsymbol{\xi}}{\boldsymbol{\xi}_{max}} \tag{4}$$

$\chi(t)$ is 0 before the chemical reaction starts and becomes 1 when the limiting reactant has completely disappeared. If the reaction is not complete, $\chi(t) \rightarrow 1$, depending on the trend of n_{L0} limiting reagent.

The amount of any chemical components in the reaction mixture at any time t is given in the following eq 5:

$$\Delta\mathbf{N} = \mathbf{N} - \mathbf{N}^0 = \boldsymbol{\xi}_{\max}\cdot\boldsymbol{\chi}\cdot\boldsymbol{\nu} = \boldsymbol{\xi}_{\max}\cdot\frac{\boldsymbol{\xi}}{\boldsymbol{\xi}_{\max}}\cdot\boldsymbol{\nu} \tag{5}$$

Rewriting eq 5, one can obtain the concentration for any species in the system with volume V_L, eq 6, respectively:

$$\mathbf{C} = (\mathbf{N}^0 + \boldsymbol{\xi}_{\max}\cdot\boldsymbol{\chi}\cdot\boldsymbol{\nu})\cdot\mathbf{V}_L^{-1} \tag{6}$$

Note that the concentration of the product depends directly on the extent of the reaction of limiting reagent, $N^0 = 0$.

Derivation of Kinetic Parameters from the Extent of Reaction. The extent of reaction ξ cannot be used to integrate the rate equation.

Using eq 7:

$$\mathbf{c} = \mathbf{c}^0 + x\cdot\boldsymbol{\nu} \tag{7}$$

with $x = \xi/V_L$ and assuming that ξ vanishes at the initial time t_0.[36] The reaction rate can be calculated via eqs 8−10:

$$\frac{dx}{dt} = \frac{1}{\nu_i}\frac{dc_i}{dt} = \frac{1}{V_L}\frac{d\xi}{dt} \tag{8}$$

For a first-order reaction process, the rate equation takes the form:

$$\frac{dx}{dt} = kc = k(c_0 + x\cdot\nu) \tag{9}$$

For a second-order reaction process, it takes the following form, which is also valid for a third-order process:

$$\frac{dx}{dt} = k\prod_j c_j^{\alpha_j} = k\prod_j (c_{0,j} + x\cdot\nu_j)^{\alpha_j} \tag{10}$$

METHODS

Inverse Problem. In this way, the approach of the inverse reaction extent model through an eigenvalue problem is applied to identify the parameters for the chemical reaction system. The procedure can be summarized in the following steps.

FT-IR Spectroscopy Data. Let $\mathbf{A}$ $(me \times n)$ represent the consolidated spectroscopic data matrix where m denotes the number of spectra taken in one step of a batch experiment (each step has an initial condition), e indicates the number of batch steps, and n is the number of data channels associated with the spectroscopic range. On the basis of a Lambert−Beer model, $\mathbf{A}$ can be assumed to result from a linear combination (eq 1) of cell path length l $(me \times me)$, concentration matrix $\mathbf{C}$ $(me \times s)$, and the pure-component spectra matrix $\mathbf{a}$ $(s \times n)$ (where s denotes the number of observable species in the chemical mixture), and $\mathbf{E}$ $(me \times n)$ is the experimental and instrumental error (eq 11).

$$\begin{aligned}\mathbf{A} &= \mathbf{l}\cdot\mathbf{C}\cdot\mathbf{a} + \mathbf{E}\\ \mathbf{A} &= \mathbf{N}\cdot\mathbf{V}_L^{-1}\cdot\mathbf{a}\end{aligned} \tag{11}$$

Determine the Minimum Number of Observable Reactions. The equations of Jouguet−de Donder (eq 3) and Lambert−Beer (eq 11) can be modeled as a linear combination, as follows in eq 12:

$$\mathbf{A} - \mathbf{A}^0 = \mathbf{N}\cdot\mathbf{a} - (\mathbf{N}\cdot\mathbf{a})^0 = \Delta\mathbf{N}\cdot\mathbf{a} \tag{12}$$

where $\mathbf{A}^0$ represents the initial conditions (starting materials) by substituting (eq 13):

$$\mathbf{A} - \mathbf{A}^0 = \boldsymbol{\xi}\cdot\boldsymbol{\nu}\cdot\mathbf{a} \tag{13}$$

a relation with reaction extent; the stoichiometric matrix and absorbance are established in eq 13. Next, a first estimate of the number of observable reactions can be obtained from the left-hand side $(\mathbf{U}_1\cdot\boldsymbol{\Sigma}_1)$ of eq 14. Singular value decomposition[30] (SVD) will give rise to three primary matrices, where it applies again for the two primary matrices $(\mathbf{U}_1\cdot\boldsymbol{\Sigma}_1)$ that correspond to the information of the reaction extent and the stoichiometric matrix eq 14, and is a very accurate representation of the Jouguet−de Donder relation for a chemical reaction system:

$$\begin{aligned}\mathbf{A} - \mathbf{A}^0 &= \mathrm{U}_1\cdot\boldsymbol{\Sigma}_1\cdot\mathbf{V}_1^{\mathrm{T}} = (\mathrm{U}_2\cdot\boldsymbol{\Sigma}_2\cdot\mathbf{V}_2^{\mathrm{T}})\cdot\mathbf{V}_1^{\mathrm{T}}\\ \boldsymbol{\xi}\cdot\boldsymbol{\nu} &= \mathbf{U}_1\cdot\boldsymbol{\Sigma}_1 = \mathbf{U}_2\cdot\boldsymbol{\Sigma}_2\cdot\mathbf{V}_2^{\mathrm{T}}\\ \mathbf{a} &= \mathbf{V}_1^{\mathrm{T}}\end{aligned} \tag{14}$$

The information contained in $\boldsymbol{\Sigma}_2$ is directly associated with the number of eigenreaction, which is analyzed by eigenvalue analysis (square of singular value $\boldsymbol{\Sigma}_2$), as can be seen as a repetitive exploratory analysis of a set of data subwindow matrices obtained from evolutionary process to determine the significant number of factors.[37] This is proportional to the rank of matrix and the chemical information contained, which can be associated with the number of observable reactions, as has been exhaustively discussed by different authors.[37−40] According to the Amrhein[38] formulation, the minimum rank for difference spectra (ΔA) matrix eq 15:

$$\mathrm{rank}\,(\Delta\mathbf{A}) = \min(\text{no. of reactions}, \text{no. of absorbing species} - 1) \tag{15}$$

This can be expressed in another form, eq 16:[37,38]

$$\mathrm{rank}\,(\Delta\mathbf{A}) = \min(\text{no. of } \xi, \text{no. of absorbing species} - 1) \tag{16}$$

If the system contains s chemical species, there will be s differential rate equations, of which $s - 1$ are independent. One of the eigenvalues will be zero (corresponding to one of the rate equations being not independent); the remaining $s - 1$ eigenvalues are functions of the rate constant.[41−43]

Determine the Change of Moles. From eqs 12−14, it is possible to derive eq 17, which yields the relative change of moles:

$$\Delta\hat{\mathbf{N}} = \boldsymbol{\xi}\cdot\boldsymbol{\nu} = \mathbf{U}_2\cdot\boldsymbol{\Sigma}_2\cdot\mathbf{V}_2^{\mathrm{T}} \tag{17}$$

A material balance criterion can be employed to construct an invariant reaction model, which optimizes a diagonal weighting matrix. $\mathbf{F}$ is required to scale this into their real magnitude in eq 18.

$$\Delta\mathbf{N} = \Delta\hat{\mathbf{N}}\cdot\mathbf{F}^{-1} = \hat{\boldsymbol{\xi}}\cdot\hat{\boldsymbol{\nu}}\cdot\mathbf{F}^{-1} \tag{18}$$

where $\mathbf{F}$ $(s \times s)$ is

$$\mathbf{F} = \begin{bmatrix} f_1 & 0 & 0 & 0\\ 0 & \ldots & 0 & 0\\ 0 & 0 & \ldots & 0\\ 0 & 0 & 0 & f_n \end{bmatrix}$$

For this reason, one needs to explain any available *a priori* information on the model parameters, to solve an *ill-posed*

problem, eq 19.

$$\Delta\tilde{\mathbf{N}} = \Delta\mathbf{N}\cdot\boldsymbol{\upsilon} \tag{19}$$

$\Delta\mathbf{N}$ and $\boldsymbol{\upsilon}$ are matrices with additional information about the extent of the model and the chemical group,[44] respectively. The consideration for defining suitable chemical groups for a reaction system is that the moles of these chemical groups must be conserved; that is, their internal elemental composition is preserved, during the chemical reaction. Obviously, the chemical species associated with the chemical group should be deduced or be observable using in the present case in situ FT-IR/ATR spectroscopy.

An *a priori* prerequisite for using this chemical group mole balance numerical optimization is that the molecular formula of the observed chemical species must be known or deduced, so the chemical group matrix $\boldsymbol{\upsilon}$ can be written for all s number of observable chemical species with g number of chemical groups. $\boldsymbol{\upsilon}$ is the generalized mass balance matrix that reduces to the typically known atomic matrix if only elemental balances are considered according to Yin and Garland and co-workers.[44]

A classical least-squares minimization applied as Tikhonov regularization process of the difference between estimated change of moles (or chemical groups) $\Delta\tilde{\mathbf{N}}$ and the actual initial moles of each elements or chemical groups existing in the system $\tilde{\mathbf{N}}^{0\rightarrow p} = \boldsymbol{\iota}\cdot\mathbf{N}^{0\rightarrow p}\cdot\boldsymbol{\upsilon}$, where $\boldsymbol{\iota}$ $(me \times 1)$ is a vector with m elements of unit value to account for the me number of spectra acquired for e batch step, and $\mathbf{N}^{0\rightarrow p}(1 \times s)$ is a vector with initial moles of the starting material in negative value to express the moles consumed in direction to the products, can be performed to solve eq 20:

$$\Delta\mathbf{N}_{res} = \left\| \Delta\tilde{\mathbf{N}} - \tilde{\mathbf{N}}^{0\rightarrow p} \right\|^2 \rightarrow \min \tag{20}$$

which is used as an objective function to determine the respective diagonal weighting factor f ($\Delta\mathbf{N}_{res}$ is a residual). Having determined the respective factor, the real change of moles can be determined from eq 18.

The minimization of the cost function eq 20 is performed by global optimization called simulated annealing (SA) according to Kirkpatrick and Corana,[45] who proposed SA in the area of combinatorial optimization; that is, they used SA in the cost function as defined in a discrete domain. This stochastic method is based on random evaluations of the cost function, to find the global minimum. Briefly, SA proceeds iteratively; it starts from a given point $\Delta\mathbf{N}_0$, and then it generates a succession of points: $\Delta\mathbf{N}_0$, $\Delta\mathbf{N}_1$, ..., $\Delta\mathbf{N}_n$, tending to the global minimum of the cost function. New candidate points are generated around the current point $\Delta\mathbf{N}_n$ applying random movements along each coordinate direction, in turn. The new coordinate values are uniformly distributed in intervals centered around $(\Delta\mathbf{N} + \delta\Delta\mathbf{N})$, the corresponding coordinate of $\Delta\mathbf{N}_n$. If the point falls outside the definition domain of $\| \Delta\tilde{\mathbf{N}} - \tilde{\mathbf{N}}^{0\rightarrow p} \|^2$, a new point is randomly generated until a point belonging to the definition domain is found. A candidate point $\Delta\mathbf{N}'$ is accepted or rejected according to the Metropolis criterion.[46] (1) A description of possible system configurations, the $\Delta\mathbf{N}_n$ are numbered $i = 0...N - 1$. A configuration is a permutation of the number $i = 0...N - 1$, interpreted as the order in which the $\Delta\mathbf{N}_n$ are calculated. (2) A generator random changes in the configuration, a procedure for taking a random step from $\Delta\mathbf{N}$ to $\Delta\mathbf{N} + \delta\Delta\mathbf{N} = \Delta\mathbf{N}'$. (3) An objective function is the simplest form of the problem whose minimization is the goal of the procedure $\Delta\mathbf{N}$ taken just as the total distance between the experimental data and the model, and (4) a control parameter T (analogue of temperature) and an *annealing schedule* that tells how it is lowered from high to low values, for example, after how many random changes in configuration is each downward step in T taken, and how large is that step.

Therefore, the objective function must be $\Delta\mathbf{N}_{res} = \| \Delta\tilde{\mathbf{N}} - \tilde{\mathbf{N}}^{0\rightarrow p} \|^2 \leq 0$, and the reaction extent is $\boldsymbol{\xi} \geq 0$ in the definition domain $\Delta\mathbf{N}_{res}$. Applied positive matrix factorization is according to Paatero and Seung.[47] In each iteration of this method, the element of $\boldsymbol{\xi}$ is multiplied by factors. As the zero elements are not updated, all of the components of $\boldsymbol{\xi}$ are strictly positive in the random minimization process. Next, in the random changes processes (2), a new point is accepted: $\Delta\mathbf{N} + \delta\Delta\mathbf{N} = \Delta\mathbf{N}'$, or else a new point is accepted with probability

$$\Pr\langle \Delta\mathbf{N} | \mathbf{N}^{0\rightarrow p}, \upsilon \rangle \propto e^{\delta\Delta\mathbf{N}_{res}/T}$$

where $\delta\Delta\mathbf{N} = \Delta\mathbf{N}' - \Delta\mathbf{N}_n$, and T is a parameter called temperature (4); in our case, this is called period.

At a fixed value of T, the succession of points $\Delta\mathbf{N}_0$, $\Delta\mathbf{N}_1$, ..., $\Delta\mathbf{N}_n$ is not downhill, except when $T = 0$. The SA algorithm starts at some "high" temperature T_0 given by the user.

A sequence of points is then generated until a sort of "equilibrium" is approached, that is, a sequence of points $\Delta\mathbf{N}_n$ whose average values of cost function reach a stable value as n increases. The best point reached is recorded as $\Delta\mathbf{N}_{opt}$. After thermal equilibration, the temperature T is reduced, and a new sequence of movements is made starting from $\Delta\mathbf{N}_{opt}$, until thermal equilibrium is reached again, and so on. The process is stopped at a temperature low enough that no more useful improvement can be expected; according to a stopping criterion, the value of $\Delta\mathbf{N}_{res} \approx 10^{-5}$. The SA optimization algorithm can be considered to be analogous to the physical process by which a material changes a state while minimizing its energy.

Determination of the Extent of Reaction, the Reaction Stoichiometries, and the Concentrations of Any Species in the System. The estimates of the real changes of moles are subjected to a SVD, eq 21:

$$\Delta\mathbf{N} = \mathbf{N} - \mathbf{N}^0 = \boldsymbol{\xi}\cdot\boldsymbol{\nu} = \mathbf{U}\cdot\boldsymbol{\Sigma}\cdot\mathbf{V}^{\mathrm{T}} \tag{21}$$

The matrix product $\mathbf{U}\cdot\boldsymbol{\Sigma}$ contains information associated with the observed extent of reaction $\boldsymbol{\xi}$ space, and $\mathbf{V}^{\mathrm{T}}$ contains the basis vector for the observed stoichiometric $\boldsymbol{\nu}$ space. A way to test the validity of the extent of reaction and the stoichimetric matrix can be inferred according to Bonvin and Rippin;[48] using reaction extents for the estimation of reaction stoichiometry without kinetic constraint, the matrix transformation $\mathbf{T}$ is required to rotate the abstract information to real information, eq 22.

$$\Delta\mathbf{N} = \xi\cdot\mathbf{T}^{-1}\cdot\mathbf{T}\cdot\boldsymbol{\nu} = \mathbf{U}\cdot\boldsymbol{\Sigma}\cdot\mathbf{V}^{\mathrm{T}} \tag{22}$$

This rotation is performed on one vector at a time using target factor analysis (TFA).[49] In this context, TFA attempts to find a match between the proposed or target stoichiometry, $\boldsymbol{\nu}_{target}$, and the abstract stoichiometries. The projected stoichiometry vector, $\boldsymbol{\nu}_{projected}$, and vector transformation $\mathbf{t}$ can be generated from a least-squares approach, eqs 23 and 24:

$$\mathbf{t} = (\boldsymbol{\nu})_{target}\cdot\mathbf{V}^{\mathrm{T}}\cdot(\mathbf{V}\cdot\mathbf{V}^{\mathrm{T}})^{-1} \tag{23}$$

$$(\boldsymbol{\nu})_{\text{projected}} = \mathbf{t}\cdot\mathbf{V}^{\mathrm{T}} \tag{24}$$

The application of the TFA technique requires special attention when linearly dependent stoichiometries occur, such as reversible reaction. Indeed, TFA will accept any linear combination of stoichiometries present in the system. This may lead to difficulties in discriminating dependent reactions. The matrix $\boldsymbol{\nu}_{\text{target}}$ must be full rank. To overcome this problem Amrhein and Brendel et al. proposed the decomposition of the stoichiometric matrix $\boldsymbol{\nu}$ as follows:[50]

$$\boldsymbol{\nu} = \mathscr{T}\cdot\boldsymbol{\nu}^{i} \tag{25}$$

where $\boldsymbol{\nu}^{i}$ is the independent stoichiometric matrix, $(R_{\mathrm{N}} \times s)$ is a full rank matrix that contains the number of reactions R_{N} linearly independent stoichiometries per s species, and $\mathscr{T}$ total reaction matrix $(R \times R_{\mathrm{N}})$ is a full rank matrix that contains the number of total reactions per R_{N}. The definition reads "*A set of reactions is said to be independent if both the stoichiometries and the kinetics are linearly independent (on the time interval* $[\mathbf{t}_0, \mathbf{t}_n]$*), and the stoichiometries are constant.*"[50] This transformation uses the concept of independent reactions for the reaction term that expresses the reactant consumption and product formation. Rewriting eqs 23 and 24 using $\boldsymbol{\nu}^{i}$ for the application of TFA:

$$\mathbf{t}^{i} = \boldsymbol{\nu}^{i}_{\text{target}}\cdot\mathbf{V}^{\mathrm{T}}\cdot(\mathbf{V}\cdot\mathbf{V}^{\mathrm{T}})^{-1} \tag{26}$$

$$\boldsymbol{\nu}_{\text{projected}} = \mathbf{t}^{i}\cdot\mathbf{V}^{\mathrm{T}} \tag{27}$$

if target stoichiometries are consistent with the observations and lie in the observed stoichiometric space. Hence, it can be seen that the target and projected stoichiometries are identical.[44,48] On the other hand, if the target is not consistent with the observations, its projection will differ from the target, and the target must be rejected. The set of possible target stoichiometries can be obtained or deduced from chemical reasoning or from an approach proposed by Bastin or Brendel et al.[39,50]

Determination of the Kinetic Constants. The parameter identification for the chemical reaction system is based on the comparison between experimental data and simulations. Consider the nonlinear least-squares minimization problem between the scaled information for reaction extent model and the simulation (based on an ordinary differential equation ODE), to fit the kinetic parameter eq 28.

$$\begin{aligned}\mathbf{Q}_{\text{res}} &= \left\| \Delta\mathbf{N}_{\text{data}} - \Delta\mathbf{N}(k)_{\text{simulate}} \right\|^{2} \\ &= \left\| [\mathbf{I} - ([\xi(k)\cdot\nu]\cdot[\xi(k)\cdot\nu]^{+})_{\text{simulate}}]\Delta\mathbf{N}_{\text{data}} \right\|^{2} \rightarrow \min\end{aligned} \tag{28}$$

Briefly, the objective of nonlinear least-squares problem using the Newton−Gauss−Marquardt (NGM)[29,30,51] method is to minimize the residual in eq 28. In this way, the aim of this fit method is to determine a vector of parameter shifts, $\Delta k = k_{\text{new}} - k_{\text{old}}$, which moves $\mathbf{Q}(k_0 + \Delta k)$ toward zero, where k_0 is the vector of initial parameter estimates. $\mathbf{q}(k_0) = -\Delta k\mathbf{J}$ is the standard definition of a single Newton−Gauss step in a form that can be solved by linear least-squares, where $\mathbf{J}$ is the Jacobian matrix.

During the iterative adjustment of the model parameters, k, the NMG method requires an estimate of the matrix of vectorized partial derivates, $\mathbf{q}(k_0)$ of $\mathbf{Q}$ as a function of the adjustable parameter, $\partial\mathbf{Q}(k_0)/\partial k$. These partial derivates are numerically approximated; one rate constant is determined in each optimization by the classic method forward finite difference.

The residuals matrix for each partial derivate is unfolded into a long column vector, $\mathbf{q}(k_0)$, and then assembled into the matrix of vectorized residuals called the Jacobian matrix, $\mathbf{J}$.

The vector containing the intrinsic rate constants k_{new} was iteratively updated from the previous vector, k_{old}, as: $k_{\text{new}} = k_{\text{old}} + (\mathbf{J}_{\mathrm{Q}}^{\mathrm{T}}\mathbf{J}_{\mathrm{Q}} + \delta\cdot\mathbf{I})^{-1}\cdot\mathbf{J}_{\mathrm{Q}}^{\mathrm{T}}\cdot q(k_0)$, where $\mathbf{J}_{\mathrm{Q}}$ is the Jacobian matrix of $\mathbf{Q}$ residuals at k_{old}, $\mathbf{I}$ is the identity matrix, δ is a scalar that assures that $\mathbf{Q}(k_{\text{new}}) \leq \mathbf{Q}(k_{\text{old}})$ and makes the minimization algorithm immune to possible singularities of $(\mathbf{J}_{\mathrm{Q}}^{\mathrm{T}}\mathbf{J}_{\mathrm{Q}})^{-1}$, and $\mathbf{q}(k_0)$ is a vector containing the residual of term in eq 28. The convergence was declared when $\mathbf{Q}_{\text{res}}$ is changed by less than $\sim 10^{-5}$.

After the adjustment of the kinetic model candidate (by ODE) to the reaction extent model, finally, the kinetic constants are obtained.

As a result, a decrease in the overall error occurs, which is reduced by nonlinear least-squares minimization and the change of moles to concentration matrix by reaction extent model optimization with the constraints mentioned below.

Other than in the case of the typical reaction extent model approach, the scoring function and driving grid-search minimization (χ^2-fitting) are based on the real experimental data set $(\Delta A_{\text{exp}})_{\text{np,ns}}$ and the corresponding error $(\sigma_{\text{exp}})_{\text{np,ns}}$:[52]

$$\chi^{2} = \left[\frac{\sum_{\text{np}}\sum_{\text{ns}} \left(\frac{(\Delta A_{\text{exp}} - \Delta A_{\text{calc}})}{\sigma_{\text{exp}}} \right)^{2}_{\text{np, ns}}}{\text{np} \times \text{ns}} \right]^{0.5} + \alpha \times \sum_{n} \left[\frac{(\xi_{\text{data}} - \xi_{\text{cal}})^{2}}{\xi_{\text{data}}} \right] \tag{29}$$

The $(\Delta A_{\text{calc}})_{\text{np,ns}}$ is calculated by reconstruction from the minimization process between the reaction extent model and the kinetic model candidate. Here, np and ns represent the number of spectra and the number of points, respectively. ξ_{data} is the concentration matrix calculated by the reaction extent model for each species n, and ξ_{cal} is the concentration calculated for each species from the kinetic rate constants. The α is a regularization parameter, which balances both minimization goals. It is a factor accounting for the differences in magnitude of the error in the spectra and the error in the concentrations. On the basis of probability considerations, the value of α should be taken as the square of the ratio of the expected error of both terms: $\alpha = (\sigma_{\mathrm{k}}/\sigma_{\mathrm{Cexp}})^{2}$. σ_{k} is taken as the average standard error of (k), as provided by the kinetic fitting mentioned above, that is, $\sim(0.03-0.4)$. We assigned a value for σ_{Cexp} of $\sim(0.12-0.1)$. The error is mainly determined by the concentration of each species, whereas the reason for the incorporation of an error due to the concentration matrix is to help to guide the reaction extent model in the right direction.

The general optimization process is summarized in the following steps:

(1) Estimation of scaling factor for the determination of reaction extent and reaction stoichiometries by minimization of eq 20.

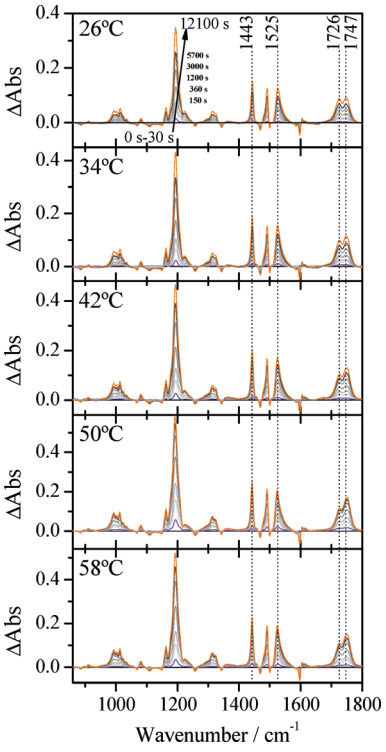

Figure 1. Time-resolved FT-IR/ATR difference spectra (preselected for easy visualization) of the reaction of phenol and phenylisocyanate to diphenyl urethane at 26, 34, 42, 50, and 58 °C.

(2) TFA is used as a validation test for the correct determination of the stoichiometric model.

(3) The kinetic rate constants k and equilibrium constants K_{eq} are estimated from eq 28 and χ^2-fitting, by minimization process between the scaled information of reaction extent model and the kinetic model candidate.

Finally, the concentration and the pure spectrum for each species can be calculated by eq 30:

$$\mathbf{C} = (\mathbf{N}^0 + \boldsymbol{\xi}_{max}\cdot\boldsymbol{\chi}\cdot\boldsymbol{\nu})\cdot\mathbf{V}^{-1} = (\mathbf{N}^0 + \boldsymbol{\xi}\cdot\boldsymbol{\nu})\cdot\mathbf{V}^{-1}$$
$$= (\mathbf{N}^0 + \Delta\mathbf{N})\cdot\mathbf{V}_L^{-1}\mathbf{a} = \mathbf{C}^+\cdot\Delta\mathbf{A} \quad (30)$$

where $\mathbf{C}^+$ represents the pseudoinverse matrix of $\mathbf{C}$, and $\Delta\mathbf{A}$ represents the difference spectra matrix.

EXPERIMENTAL SECTION

Materials and Spectroscopy. The reaction (Figure 1) was performed in a 250 mL four-necked round-bottom flask with a reflux condenser and a magnetic stirrer. Two quick-fits were used for the ATR probe, and the contact thermometer controlling the reaction temperature and the fourth opening was used for the addition of the chemicals. For the reaction, 9.88 g (1.05 mol L^{-1}) of phenol was dissolved in chloroform, and after addition of 0.3 g of anhydrous $AlCl_3$ catalyst,[33] this solution was heated to the respective reaction temperature (26, 34, 42, 50, and 58 °C). When the reaction temperature was reached, a spectrum was recorded, and subsequently 11.91 g (1.00 mol L^{-1}) of phenyl isocyanate was added to this mixture.

The spectroscopic measurements were performed on a Bruker IFS-28 FT-IR spectrometer (Bruker Optik GmbH, Ettlingen, Germany) equipped with an MCT detector and a diamond ATR-probe (two reflections), which was coupled to the spectrometer by a 2 m silver halide waveguide-fiber (Infrared Fiber Sensors, Aachen, Germany).[11] IR spectra were recorded in preselected time intervals (matrix of 29 × 488) at a spectral resolution of 4 cm^{-1}, and 32 scans were accumulated for the improvement of the signal−noise ratio.

Computational Methods. SVD was performed using the linear algebra package library (LAPACK for Windows), and all calculations of ordinary differential equations are solved by ODE45, Runge−Kutta integrated numerically using with matlab functions. Newton−Gauss−Marquardt is according to Kelley, Teukolsky et al., and Lórenz-Fonfría algorithms,[29,30,51] global optimization by simulated annealing is according to Kirkpatrick and Corana,[45] and non-negativity constraint is according to Paatero and Seung,[47] TFA is based on in Malinowski code;[49] all calculations were performed in a homemade program written in MATLAB version 7 (The Math Works, Natick, MA).

RESULTS AND DISCUSSION

Spectral Analysis. Figure 1 displays the FT-IR/ATR difference spectra (constructed by subtraction of the initial condition A^0) for the reaction of phenyl isocyanate and phenol to diphenyl urethane in chloroform solution at 26, 34, 42, 50, and 58 °C. A prominent doublet of the hydrogen-bonded and the free ν(C═O) absorption bands at 1726 and 1747 cm^{-1}, respectively, is formed. The amide II (ν(C═O) + δ(NH)) absorption is located at 1525 cm^{-1}, and the evolution of the reaction product was characterized by the appearance of an absorption at 1443 cm^{-1}.[33] The 1443 cm^{-1} absorption band has been assigned to a partial C═N double bond in conjugation with the aromatic ring vibrations of the isomeric structure of diphenyl urethane (DPhU in Scheme 1).[33] However, the observed changes in the wavenumber region of 1800−1700 cm^{-1}, especially the non-hydrogen-bonded ν(C═O) absorption band at 1747 cm^{-1}, show a stronger intensity with increasing temperature. To determine the number of observable reactions, the eigenvalue analysis has been applied to the data matrices at different temperatures.

Determination of the Number of Reactions. The number of reactions was determined by eigenvalue analysis from SVD performed on the $[\mathbf{A} - \mathbf{A}^\circ]$ difference spectroscopy matrix. Figure 2 shows the eigenvalues (in log units) as a function of the position of the considered row in the data matrix (row number), which corresponds to the time direction. Two eigenvalues or factors are significant for each experiment at 26, 34, 42, 50, and 58 °C for this analysis. A threshold separating minor contributions can be set at ∼−3.42 (26 °C), −4.31 (34 °C), −4.5 (42 °C), −4.42 (50 °C), and −4.41 (58 °C) (in log units) for the two factors.

Two contributions emerge at the same time, from the beginning of the reaction, showing a high variability in the initial time interval between 0 and 1500 s. This number is consistent with the Amrhein[38] formulation to predict the number of reactions.

We can infer that this contribution is related to two processes, correlating with the formation of the isomeric structures of the diphenyl urethane in equilibrium. One factor is interpreted as a contribution of the synthesis of diphenyl urethane, and the other factor is a contribution of diphenyl urethane in equilibrium

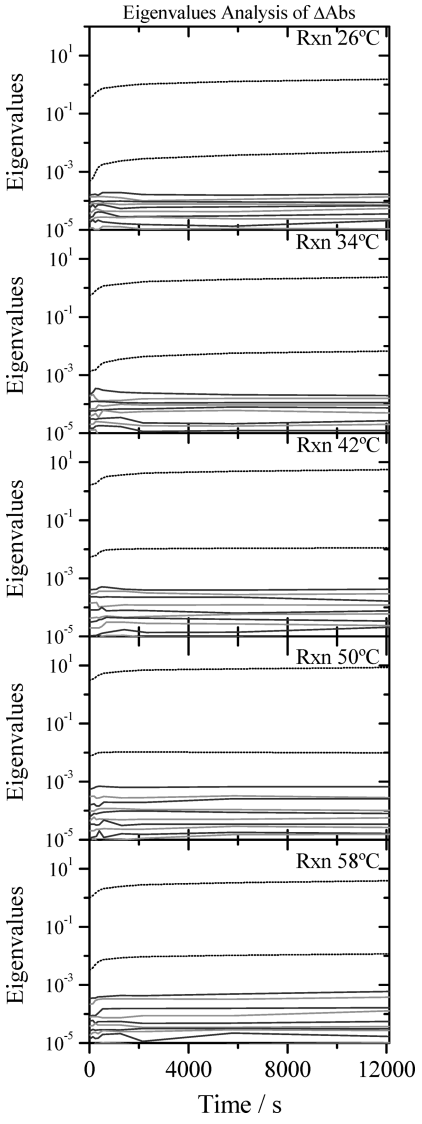

Figure 2. Eigenvalue analysis for the time-resolved FTIR difference spectra at 26, 34, 42, and 58 °C (eigenvalue, assigned to factors (----) and noise (—)).

between the free form and the form with hydrogen bonds. This is related to the postulation of a kinetic reaction with the following model (Scheme 2).

Changes in Moles, Extent of Reaction, and Reaction Stoichiometry Matrix. On the basis of the knowledge of the eigenvalue analysis and the amount of initial moles of reactants, a reaction invariant model was set up to calculate the real change of moles according to the minimization of eq 20. In our case, we implement the concept of limiting reagent for the calculation of changes of moles (eq 5). Because the concept of functional group matrix cannot be used alone, the general eq 17 can be rewritten as eq 28:

$$\Delta\hat{\mathbf{N}} = \boldsymbol{\xi}\cdot\boldsymbol{\nu} = \sum_{i=1}^{m}\xi_i\cdot\nu_i = \sum_{i=1}^{m}\mathbf{u}_{2i}\cdot\boldsymbol{\varepsilon}_{2i}\cdot\mathbf{v}_{2i}^{\mathrm{T}} = \mathbf{U}_2\cdot\boldsymbol{\Sigma}_2\cdot\mathbf{V}_2^{\mathrm{T}}$$

$$\text{subject to}: 0 \le \xi_i \le \xi_{\max} = \frac{n_{iL0}}{\nu_i}, \chi = \frac{\xi_i}{\xi_{\max}} \rightarrow 1 \qquad (31)$$

Scheme 2. Reaction of Phenol and Phenyl Isocyanate to Diphenyl Urethane and the Isomeric Structures of the Diphenyl Urethane

$$\mathrm{PhOH} + \mathrm{PhNCO} \xrightarrow{k_t} \mathrm{DPhU_{Total}}$$

$$\mathrm{DPhU} \underset{K_d=k_t/k_f}{\overset{K_a=k_t/k_r}{\rightleftarrows}} \mathrm{DPhUH_{eq}}$$

The reaction advancement ratio χ is added, and it is proportional to $\xi_i = \xi_{\max}\chi$. As explained above, when the limiting reactant has completely disappeared, $\xi \rightarrow \xi_{\max}$ ($\chi \rightarrow 1$). This condition contributes to improve the optimization process.

In the present synthesis of diphenyl urethane, the concept of functional group matrix proposed by Garland and co-workers[44] is modified to include molecular interaction information. Note that the final products have the same functional groups ν(C═O), and these cannot be used alone.

However, fortunately one can use the significant difference in the molecular interaction between the hydrogen-bonded and the free diphenyl urethanes for ν(C═O) and C═N double bond in conjugation with the aromatic ring present free form of diphenyl urethane. The concept of molecular interaction is useful and will be used throughout. Thus, a molecular interaction matrix $\boldsymbol{\upsilon}$ is constructed as follows, with row species and column functional groups and molecular interaction. "0" means no functional group in this species, 1 corresponds to the functional groups (g), −OH, N═C═O, C═O, and C═N, in this species, and finally 1 corresponds to the functional groups, C═O−H, with molecular interaction (gmi), respectively.

$$\boldsymbol{\upsilon} = \begin{array}{c} \begin{matrix} \mathrm{OH} & \mathrm{NCO} & \mathrm{COH} & \mathrm{CO} & \mathrm{CN} \end{matrix} \\ \begin{bmatrix} 1 & 0 & 0 & 0 & 0 \\ 0 & 1 & 0 & 0 & 0 \\ 0 & 0 & 1 & 0 & 0 \\ 0 & 0 & 0 & 1 & 1 \end{bmatrix} \end{array} \begin{matrix} \mathrm{PhOH} \\ \mathrm{PhNCO} \\ \mathrm{DPhUH} \\ \mathrm{DPhU} \end{matrix}, \mathrm{s} = 4, \mathrm{g} = 4, \mathrm{gmi} = 1$$

Their inclusion in the $\mathbf{F}_{s\times s}$ ($s \times s$ is species per species) optimization is important, because a difference spectra full range fitting is performed using multiple linear regression to estimate the change of moles.

The number of decision variables in the diagonal matrix $\mathbf{F}_{s\times s}$ is 4, and these correspond (equation of change of moles) to PhOH, PhNCO and DPhU, DPhUH. The weightings for the four components (in the diagonal matrix) were assigned arbitrarily numbers of a proper magnitude to prevent matrix *ill-conditioning*. Also applied is a non-negative matrix factorization as a non-negative constraint based on the positive matrix factorization according to Paatero and Seung.[46]

The scaling factor in the diagonal matrix $\mathbf{F}_{s\times s}$ can be estimated by imposing a closure constraint on the mole balance according to eq 2 and the concept of limiting reagents (eq 5) for the calculation of change of moles, using stochastic global optimization method. The successful determination of the spectral scaling factor depends, to the significant extent, on whether the system is closed for a particular chemical group. If the system is open, it is not possible to obtain the correct scaling factor. The scaling factor in the diagonal matrix $\mathbf{F}_{s\times s}$ is presented

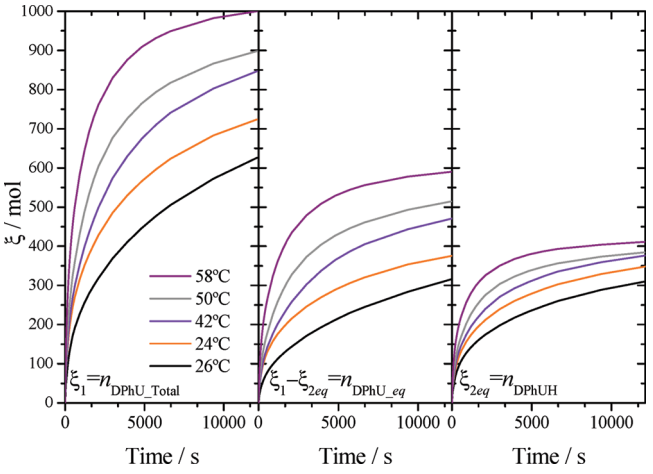

Figure 3. The curves for the extent ξ_1 of PhOH + PhNCO → $DPhU_{total}$, reaction extent ξ_{2eq} of equilibrium DPhUH, and difference of reaction extent $\xi_1 - \xi_{2eq}$ are proportional to DPhU in the equilibrium.

as follows:

$$\text{diag } \mathbf{F} = \begin{bmatrix} f_{1,1}^{\text{PhOH}} \\ f_{2,2}^{\text{PhNCO}} \\ f_{3,3}^{\text{DPhU}} \\ f_{4,4}^{\text{DPhUH}} \end{bmatrix}; \text{diag } \mathbf{F}^{26^\circ\text{C}} = \begin{bmatrix} f_{1,1}^{\text{PhOH}} \\ f_{2,2}^{\text{PhNCO}} \\ 0.9070 \\ 0.8194 \end{bmatrix};$$

$$\text{diag } \mathbf{F}^{34^\circ\text{C}} = \begin{bmatrix} f_{1,1}^{\text{PhOH}} \\ f_{2,2}^{\text{PhNCO}} \\ 0.9381 \\ 0.9997 \end{bmatrix}; \text{diag } \mathbf{F}^{42^\circ\text{C}} = \begin{bmatrix} f_{1,1}^{\text{PhOH}} \\ f_{2,2}^{\text{PhNCO}} \\ 0.8576 \\ 0.8137 \end{bmatrix};$$

$$\text{diag } \mathbf{F}^{50^\circ\text{C}} = \begin{bmatrix} f_{1,1}^{\text{PhOH}} \\ f_{2,2}^{\text{PhNCO}} \\ 0.9662 \\ 0.9017 \end{bmatrix} \text{diag } \mathbf{F}^{58^\circ\text{C}} = \begin{bmatrix} f_{1,1}^{\text{PhOH}} \\ f_{2,2}^{\text{PhNCO}} \\ 0.9141 \\ 0.8511 \end{bmatrix},$$

$$f_{1,1}^{\text{PhOH}} = f_{3,3}^{\text{DPhU}} + f_{4,4}^{\text{DPhUH}}$$
$$f_{2,2}^{\text{PhNCO}} = f_{3,3}^{\text{DPhU}} + f_{4,4}^{\text{DPhUH}}$$

The minimization of the sum of squared error function for the global optimization was performed using the simulated annealing method of Kirkpatrick and Corana.[45]

The extent of reactions was calculated using eq 21, and their values for each observation in the batch process are presented in Figure 3. The results show that the advancement for the reaction ξ_1 is associated with the synthesis of diphenyl urethane for different temperatures, corresponding to the total moles of product. The other reaction extent ξ_2 is associated with the equilibrium of the diphenyl urethane, corresponding to the number of moles of diphenyl urethane with hydrogen bonds. The difference in the reaction extents $(\xi_1 - \xi_2)$ is proportional to the number of moles of diphenyl urethane in the free form. It is noted that the equilibrium is displaced to the free form of diphenyl urethane with increasing temperature, as expected.

Reaction Stoichiometric Matrix. The changes of moles of PhOH, PhNCO, DPhU, and DPhUH were calculated using eq 21, where $\mathbf{N}^0$ denotes initial moles of reagent (first spectrum) for the experiments at different temperatures. SVD was performed on $\Delta\mathbf{N}$, and the diagonal values of the singular matrix $\mathbf{\Sigma}_2$ are presented as follows:

$$\text{diag } \mathbf{\Sigma}_2^{26^\circ\text{C}} = \begin{bmatrix} 0.0820 \\ 0.0549 \\ 0.0000 \end{bmatrix}; \text{diag } \mathbf{\Sigma}_2^{34^\circ\text{C}} = \begin{bmatrix} 0.0375 \\ 0.0279 \\ 0.0000 \end{bmatrix};$$

$$\text{diag } \mathbf{\Sigma}_2^{42^\circ\text{C}} = \begin{bmatrix} 0.0607 \\ 0.0344 \\ 0.0001 \end{bmatrix}; \text{diag } \mathbf{\Sigma}_2^{50^\circ\text{C}} = \begin{bmatrix} 0.0851 \\ 0.0683 \\ 0.0000 \end{bmatrix};$$

$$\text{diag } \mathbf{\Sigma}_2^{58^\circ\text{C}} = \begin{bmatrix} 0.0781 \\ 0.0520 \\ 0.0000 \end{bmatrix}$$

Only the first two factors of the singular matrix are significant, and therefore the number of observable reactions is equal to two. This number is consistent with the Amrhein formulation[38] and the Gibb's stoichiometric rule proposed by Aris and Mah[53] and Feinberg[54] to predict the number of independent reactions, r. This rule is represented by

$$r \leq s - p \tag{32}$$

where s is the number of components and p is the rank of the functional group matrix. However, in our case, p is the rank in the functional group matrix (for all $s \times g$ and gmi only of the products). Thus, for this reduced problem, because $s = 4$ and $p = 2$, $r \leq 2$. It should be remembered that the mathematical treatment considers two separate processes to carry out the calculations.

Target factor analysis is used to check whether the proposed reaction stoichiometries are compatible with the observation space $\mathbf{V}^T$. The set of potential target stoichiometries for the reaction network could be extracted from the chemical group matrix according to the method proposed by Yin and Garland coworkers[44] or an approach proposed by Bastin and Brendel et al.[39,50] Accordingly, the current system can be considered as one reaction, and a coupled equilibrium is represented by feasible stoichiometric candidates in a matrix form as follows:

$$\boldsymbol{\nu}_{\text{target}} = \begin{bmatrix} -1 & -1 & 1 & 0 \\ 0 & 0 & -1 & 1 \\ 0 & 0 & 1 & -1 \end{bmatrix}$$

Because of the linear dependence of the stoichiometries in the equilibrium, the decomposition of the stoichiometric matrix is applied using the concept of eq 25:[50]

$$\boldsymbol{\nu}_{\text{target}} = \begin{bmatrix} 1 & 0 \\ 0 & 1 \\ 0 & -1 \end{bmatrix} \begin{bmatrix} -1 & -1 & 1 & 0 \\ 0 & 0 & -1 & 1 \end{bmatrix} = \mathscr{T} \cdot \boldsymbol{\nu}^i$$

TFA is applied in $\boldsymbol{\nu}^i$ $(R_N \times s)$ that satisfies the condition of full rank matrix.

$$\boldsymbol{\nu}_{\text{target}}^i = \begin{bmatrix} -1 & -1 & 1 & 0 \\ 0 & 0 & -1 & 1 \end{bmatrix}$$

dx.doi.org/10.1021/jp202227d | J. Phys. Chem. A 2011, 115, 8832–8844

Upon projecting these target vectors onto the observation space $\mathbf{V}^{T}$, the projected stoichiometries are as follows:

$$\nu^{26°C}_{projected} = \begin{bmatrix} -1.0000 & -1.0300 & 0.9987 & 0.0003 \\ 0.0000 & 0.0000 & -0.9987 & 0.9976 \end{bmatrix}$$

$$\nu^{34°C}_{projected} = \begin{bmatrix} -1.0000 & -1.0000 & 0.9943 & 0.0011 \\ 0.0011 & 0.0000 & -0.9943 & 0.9995 \end{bmatrix}$$

$$\nu^{42°C}_{projected} = \begin{bmatrix} -1.0000 & -1.0000 & 0.9869 & 0.0001 \\ 0.0000 & 0.0000 & -0.9869 & 0.9971 \end{bmatrix}$$

$$\nu^{50°C}_{projected} = \begin{bmatrix} -1.0000 & -1.0000 & 0.9978 & 0.0003 \\ 0.0000 & 0.0000 & -0.9978 & 0.9975 \end{bmatrix}$$

$$\nu^{58°C}_{projected} = \begin{bmatrix} -1.0000 & -1.0000 & 0.9989 & 0.0004 \\ 0.0000 & 0.0000 & -0.9989 & 0.9992 \end{bmatrix}$$

The sum of square errors between target and projected stoichiometries for the two reactions are $\sim 10^{-5}$, respectively. By most standards, these errors are very small. Thus, it can be confidently concluded that the target vectors are the true reaction stoichiometries observed in this current system.

Concentrations, Spectra of Species, and Kinetics. By resolving the extent of reactions in each process at different temperatures, the concentration of the four species can be calculated according to eq 30. On the basis of the deconvolution from SVD and the minimization process, we represent the concentrations considered for the synthesis of diphenyl urethane and a coupled equilibrium of diphenyl urethane with and without hydrogen bonding.

In terms of mass balance, it is possible to calculate the concentration for each specie for one reaction and a coupled equilibrium as follows.

Synthesis of diphenyl urethane and a coupled equilibrium of diphenyl urethane with and without hydrogen bonds, eq 33:

$$\begin{aligned} [\mathrm{PhOH}] &= (n_0 - \xi_1 \cdot \nu) \cdot V_L^{-1} \\ [\mathrm{PhNCO}] &= (n_{L0} - \xi_1 \cdot \nu) \cdot V_L^{-1} \\ [\mathrm{DPhU}]_{total} &= (n_{0,\mathrm{DPhU}} + \xi_1 \cdot \nu) \cdot V_L^{-1} \\ [\mathrm{DPhU}]_{eq} &= (n_{0,\mathrm{DPhU}} + (\xi_1 - \xi_2) \cdot \nu) \cdot V_L^{-1} \\ [\mathrm{DPhUH}]_{eq} &= (n_{0,\mathrm{DPhUH}} + \xi_{2eq} \cdot \nu) \cdot V_L^{-1} \end{aligned} \quad (33)$$

According to eq 30, it is possible to obtain the pure spectra for the isomeric structures using eq 34:

$$\mathbf{a} = \mathbf{C}^{+} \cdot \Delta\mathbf{A} = \begin{bmatrix} (n_0 - \xi_1 \cdot \nu) \cdot V_L^{-1} \\ (n_{L0} - \xi_1 \cdot \nu) \cdot V_L^{-1} \\ (n_{0,\mathrm{DPhU}} + (\xi_1 - \xi_{2eq}) \cdot \nu) \cdot V_L^{-1} \\ (n_{0,\mathrm{DPhUH}} + \xi_{2eq} \cdot \nu) \cdot V_L^{-1} \end{bmatrix}^{+} \cdot \Delta\mathbf{A} \quad (34)$$

There is no dependency between the concentration profiles. For this reason, it is possible to separate these spectra using pseudo inverse matrix of the concentration profiles, according to Amrhein.[38]

For reasons of relevance and space, we show only the spectra of the products derived at 26 °C; similar results were also found for the other temperatures. Figure 4 shows the resolved spectra of DPhUH and DPhU for the reaction at 26 °C. It is possible to observe good resolution of bands at 1726 and 1747 cm^{-1} both due to ν(C═O) and 1443 cm^{-1} band for C═N double bond in conjugation with the aromatic ring vibrations of the isomeric structure of DPhU. It is the most distinctive characteristic between the spectra of DPhUH and DPhU.

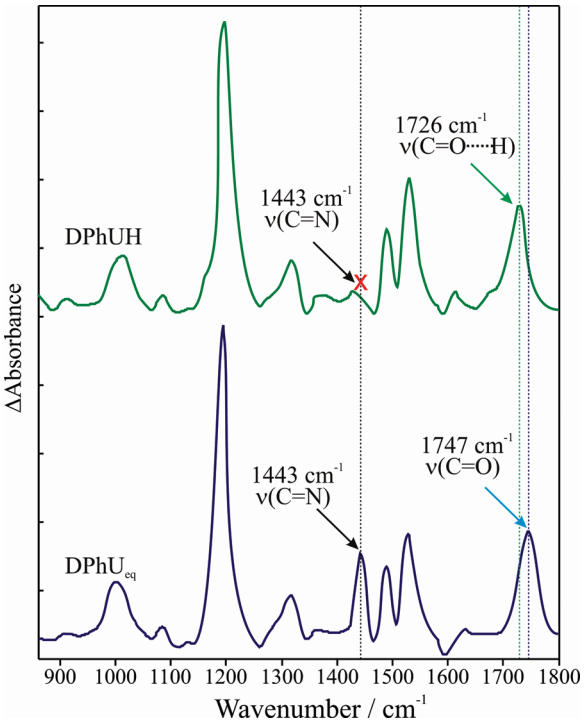

Figure 4. Plots of the resolved spectra from the reaction extent model. The spectrum for DPhUH is shown in green, with the hydrogen-bonded C═O band at 1726 cm^{-1}, and the spectrum for DPhU is in blue, with the non-hydrogen-bonded C═O band at 1747 cm^{-1}.

Figure 5 shows the concentration profiles of all species at different temperatures. The left column of Figure 5 displays the total concentrations of the reagents (PhOH, PhNCO) and diphenyl urethane species (DPhUH and DPhU). (The model for the reaction extent explains 99.7% (26 °C), 99.5% (34 °C), 99.3% (42 °C), 99.8% (50 °C), and 99.9% (58 °C) of the variance of the $\Delta\mathbf{A}$ difference spectra matrix.)

It is possible to observe a larger increment for the formation of DPhU as compared to DPhUH as a function of temperature along the reaction progress. The result is in contrast to the results obtained by Friebe and Siesler[33] where a deviation is observed in the quantification between FT-IR/ATR and HPLC. The IR data show higher concentration values for the reaction monitored at 58 °C relative to the chromatographic analysis. This can be explained through an overlap between the reaction and the equilibrium coupled occurring at the same time.

On the other hand, it can be expected at different temperatures the concentration of DPhU increases, whereas that of DPhUH should decrease, controlled by a mass balance at different temperatures. This suggests that the construction of a kinetic model for these reactions would be controlled by the global equilibrium constant.

The relative proportions between the isomeric structures are controlled for the equilibrium and are given by the ratio of the two rates and, therefore, of the two rate constants, eq 35:

$$K_a = \frac{k_f}{k_r} = \frac{(n_{0,\mathrm{DPhUH}} + \xi_{2eq} \cdot \nu) \cdot V_L^{-1}}{(n_{0,\mathrm{DPhU}} + (\xi_1 - \xi_{2eq}) \cdot \nu) \cdot V_L^{-1}} \text{ or } K_d = \frac{1}{K_a} \quad (35)$$

dx.doi.org/10.1021/jp202227d |J. Phys. Chem. A 2011, 115, 8832–8844

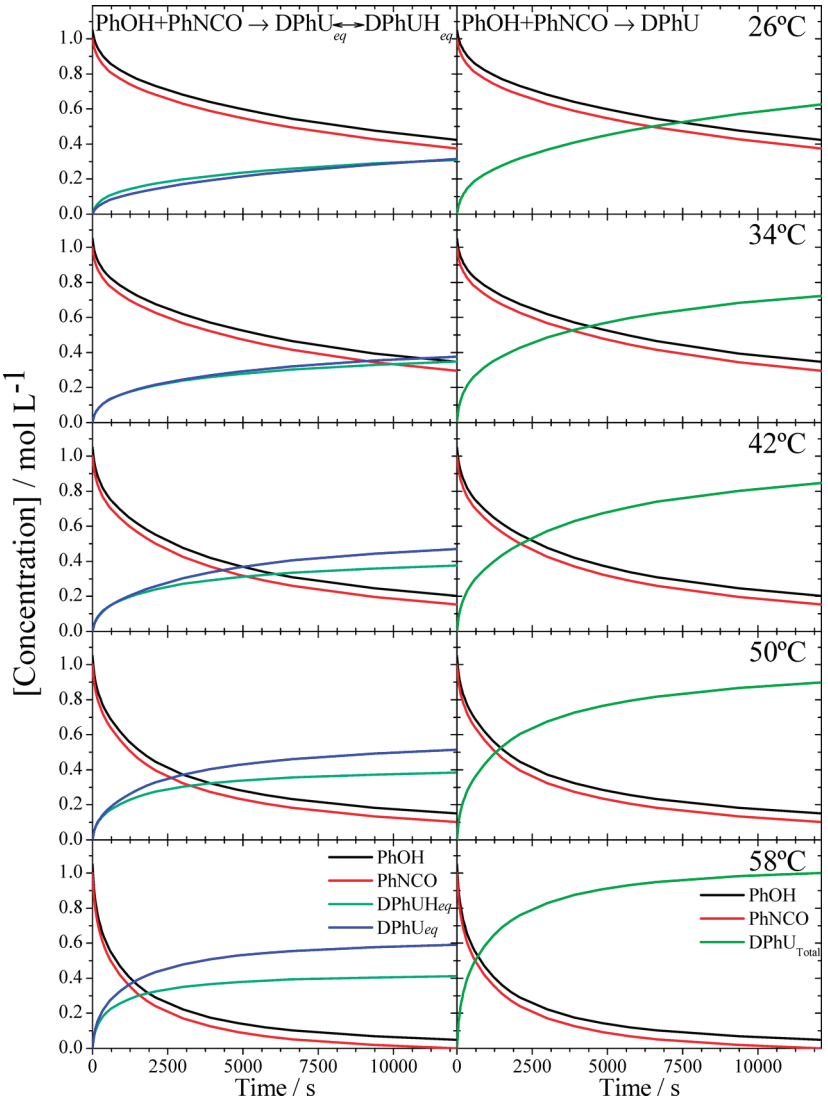

Figure 5. Concentration profiles for all species at different temperatures. The left column shows the concentration profiles of all species, the total concentrations for the reagents (PhOH, PhNCO), and the product DPhU. The right column shows the concentration profiles fitted for the species in the synthesis of hydrogen-bond and non-hydrogen-bond diphenyl urethane in the equilibrium.

The ratio presents the kinetic control over the proportion of the products, and it is a common feature of the reactions encountered in this case. Moreover, the equilibrium constant between the formation of DPhU and DPhUH represents the instantaneous interchange of the hydrogen bonding. Thus, these equilibriums are a quantification of the association and dissociation of the hydrogen bond that interacts with the two isomers. In this case, the products reach equilibrium instantaneously, the proportion of the products is determined by thermodynamics considerations, and the ratio of the concentrations is controlled by considerations of the standard Gibbs energies. On the other hand, the reagent consumption and total product formation are determined by kinetic considerations.

Assuming the dependence of the global equilibrium constant on the product, the data fitting (using eq 28) can be analyzed as one reaction and an equilibrium between the isomeric structures. This model corresponds to Scheme 2 suggested by reaction extent modeling. The ODEs based on extent of model are shown as follows:

$$d\xi_1/dt = k_1(n_0 - \xi_1 \cdot \nu)(n_{L0} - \xi_1 \cdot \nu) = k_1(n_{0,C} + \xi_1 \cdot \nu)$$
$$d\xi_{2eq}/dt = k_f(n_{0,DPhU} + (\xi_1 - \xi_{2eq}) \cdot \nu)$$
$$= k_r(n_{0,DPhUH} + \xi_{2eq} \cdot \nu) \quad (36)$$

It is possible to characterize the real concentrations of the global system of PhOH, PhNCO and DPhU, DPhUH by the kinetic and equilibrium constants k_1, $K_a = k_f/k_r$, or $K_d = 1/K_a$. In this way, one can see that k_1 describes the formation of the total mass of diphenyl urethane, while K_a describes the proportion between of the isomeric structures. The ODEs were based on the reaction extent model for the reaction and the equilibrium described in Scheme 2.

The parameters (kinetic constant and equilibrium) for the chemical reaction system based on comparison between the experimental data and the simulations are listed in Table 1. Figure 5 (right column) exhibits the concentration profiles,

Table 1. Calculated Rate, Association, and Dissociation Constants for the Synthesis of Hydrogen-Bonded (HB) and Non-Associated Diphenyl Urethane at Different Temperatures

	26 °C	34 °C	42 °C	50 °C	58 °C
DPhU k_1 ($\times 10^{-4}$ M^{-1} s^{-1})	2.31 ± 0.14	3.25 ± 0.21	3.9 ± 0.72	5.03 ± 0.29	7.53 ± 0.30
$K_{a\_HB} = k_f/k_r$	1.31 ± 0.12	0.97 ± 0.01	0.95 ± 0.05	0.84 ± 0.02	0.67 ± 0.01
$K_{d\_HB} = k_r/k_f$	0.76 ± 0.07	1.03 ± 0.16	1.06 ± 0.02	1.19 ± 0.10	1.49 ± 0.13

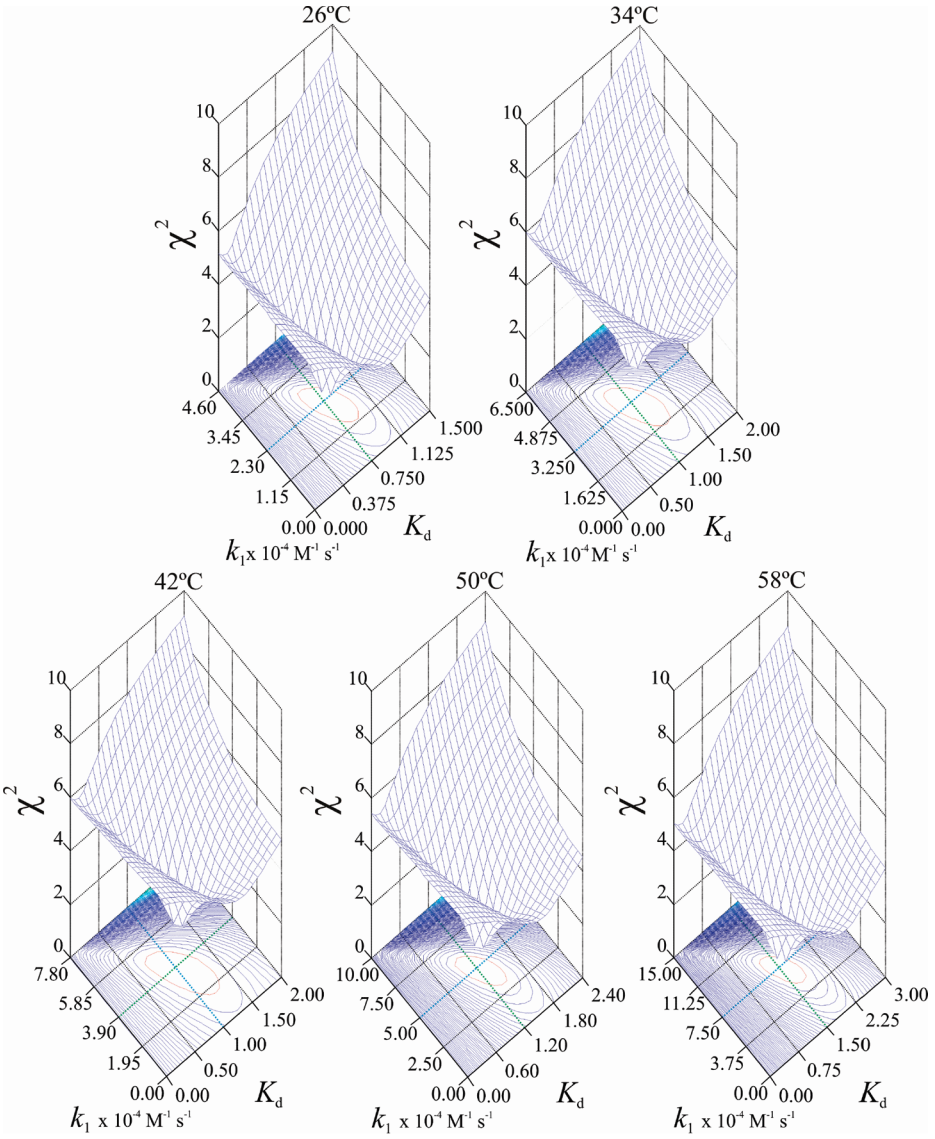

Figure 6. Two-dimensional grid search showing a minima around the expected k_1 and K_d values at different temperatures.

which are fitted ($d\xi_1/dt$) for PhOH, PhNCO, and total DPhU. Values corresponding to k_1 for the second-order reaction are calculated on the basis of eq 36.

The analysis of the equilibrium yields the kinetic constant ratio of k_f and k_r for the isomeric structures of diphenyl urethane. This allows the computation of the association and dissociation constants for the formation of hydrogen bonding of the urethane structures. An increment of K_d is observed with temperature, as may be expected from the strong dependence of hydrogen bonding on temperature. It is proportional to the formation of DPhU.

To validate the approach described in eq 29, the fitting procedure of χ^2 is presented in Figure 6, showing two-dimensional grids for the search of the minimum in a k_1 versus K_d plane at difference temperatures. In general, high sensitivity and good results for the kinetic optimization are obtained. The sharper hyperplanes of the two-dimensional grid minimum for k_1 and K_d at 26, 50, and 58 °C, as compared to the more diffuse results for the experiments at 34 and 42 °C, can be interpreted as the lack of fit for the experimental data. The kinetic and equilibrium constants k_1 and K_d for the five experiments have χ^2 values <1.50.

dx.doi.org/10.1021/jp202227d |J. Phys. Chem. A 2011, 115, 8832–8844

CONCLUSIONS

Using FT-IR/ATR spectroscopy, fiber optic mode in the synthesis of diphenyl urethane at different temperatures has been investigated by modeling the reaction extent as an inverse kinetic problem. Reliable reaction rate constant and equilibrium have been reported for the two isomers of diphenyl urethane with and without hydrogen bonding of the C═O group. Thus, the kinetic rate constant k_1 to the total species DPhU, respectively, has been identified. Furthermore, the association and dissociation constants for the hydrogen bonding of the isomeric structure of diphenyl urethane were identified. Moreover, k_f and k_r on the two isomers were determined.

The retrieved data include the number of reactions, extent of reactions, reaction stoichiometries, time-dependent concentrations, kinetics rate constants, and validation using χ^2 fitting. The results obtained here bear important advantage because they can be considered free from subjective and univariate assumptions and influences of errors arising from complicated experimental setups. Generally, this research opens the possibility of modeling the extent of the reaction and performing a kinetic analysis of the hydrogen bonding in an organic system. Important information could be extracted, which could also help to better understand different functions and interactions of hydrogen bonding in supramolecular system. This is the first comprehensive kinetic study of linked reactions and their temperature dependences in the synthesis of the isomeric structure of diphenyl urethane, by using a methodology of regularization for the inverse reaction extent model, through an eigenvalue problem to identify the parameters for the chemical reaction system.

AUTHOR INFORMATION

Corresponding Author

*E-mail: nicolas.spegazzini@gmail.com.

ACKNOWLEDGMENT

N.S. acknowledges support from the Japan Society for the Promotion of Science (JSPS) for a postdoctoral fellowship (Grant PE10056).

REFERENCES

(1) (a) Günzler, H.; Gremlich, H.-U. *IR Spectroscopy, An Introduction*; Wiley-VCH: Weinheim, 2002. (b) Siesler, H. W.; Ozaki, Y.; Kawata, S.; Heise, H. M. *Near-Infrared Spectroscopy Principles, Instruments, Applications*; Wiley-VCH: Weinheim, 2002. (c) Ferraro, J. R.; Nakamoto, K.; Brown, C. W. *Introductory Raman Spectroscopy*, 2nd ed.; Elsevier Science: Amsterdam, 2003.

(2) Heaton, B. *Mechanism in Homogeneous Catalysis, A Spectroscopic Approach*; Wiley-VCH: Weinheim, 2005; Chapter 4.

(3) Ross, J. *Acc. Chem. Res.* **2003**, *36*, 839–847.

(4) Clarke, B. L. *Adv. Chem. Phys.* **1980**, *43*, 1–215.

(5) (a) Chevalier, T.; Schreiber, I.; Ross, J. *J. Phys. Chem.* **1993**, *97*, 6776–6787. (b) Arkin, A.; Ross, J. *J. Phys. Chem.* **1995**, *99*, 970–979. (c) Ross, J. *J. Phys. Chem. A* **2008**, *112*, 2134–2143.

(6) (a) Díaz-Sierra, R.; Lozano, J. B.; Fairén, V. *J. Phys. Chem. A* **1999**, *103*, 337–343. (b) Mihaliuk, E.; Skødt, H.; Hynne, F.; Sørensen, P. G.; Showalter, K. *J. Phys. Chem. A* **1999**, *103*, 8246–8251.

(7) (a) Gemperline, P. J.; Puxty, G.; Maeder, M.; Walker, D.; Tarczynski, F.; Bosserman, M. *Anal. Chem.* **2004**, *76*, 2575–2582. (b) Puxty, G.; Neuhold, Y.-M.; Jecklin, M.; Ehly, M.; Gemperline, P. J.; Nordon, A.; Littlejohn, D.; Basford, J. K.; De Cecco, M.; Hungerbühler, K. *Chem. Eng. Sci.* **2008**, *63*, 4800–4809. (c) McCann, N.; Phan, D.; Wang, X.; Conway, W.; Burns, R.; Attalla, M.; Puxty, G.; Maeder, M. *J. Phys. Chem. A* **2009**, *113*, 5022–5029. (d) Wang, X.; Conway, W.; Burns, R.; McCann, N.; Maeder, M. *J. Phys. Chem. A* **2010**, *114*, 1734–1740.

(8) Schmitz, G.; Kolar-Anić, L. Z.; Anić, S.; Čupić, Z. D. *J. Phys. Chem. A* **2008**, *112*, 13452–13457.

(9) (a) Zogg, A.; Fischer, U.; Hungerbühler, K. *Ind. Eng. Chem. Res.* **2003**, *42*, 767–776. (b) Puxty, G.; Maeder, M.; Rhinehart, R. R.; Alam, S.; Moore, S.; Gemperline, P. *J. Chemom.* **2005**, *19*, 329–340. (c) Ehly, M.; Gemperline, P. J.; Nordon, A.; Littlejohn, D.; Basford, J. K.; De Cecco, M. *Anal. Chim. Acta* **2007**, *595*, 80–88.

(10) Visentin, F.; Puxty, G.; Kut, O. M.; Hungerbühler, K. *Ind. Eng. Chem. Res.* **2006**, *45*, 4544–4553.

(11) (a) Heise, H. M.; Kuepper, L.; Butvina, L. N. *Anal. Bioanal. Chem.* **2003**, *375*, 1116–1123. (b) Minnich, C. B.; Buskens, P.; Steffens, H. C.; Bäuerlein, P. S.; Butvina, L. N.; Küpper, L.; Leitner, W.; Liauw, M. A.; Greiner, L. *Org. Process Res. Dev.* **2007**, *11*, 94–97.

(12) Zogg, A.; Fischer, U.; Hungerbühler, K. *Chem. Eng. Sci.* **2004**, *59*, 5795–5806.

(13) Müller, J. J.; Neumann, M.; Scholl, P.; Hilterhaus, L.; Eckstein, M.; Thum, O.; Liese, A. *Anal. Chem.* **2010**, *82*, 6008–6014.

(14) Xu, L.; Li, C.; Ng, K. Y. S. *J. Phys. Chem. A* **2000**, *104*, 3952–3957.

(15) Du, Y.; George, S. M. *J. Phys. Chem. C* **2007**, *111*, 8509–8517.

(16) Bjørgen, M.; Lillerud, K.-P.; Olsbye, U.; Bordiga, S.; Zecchina, A. *J. Phys. Chem. B* **2004**, *108*, 7862–7870.

(17) Yeom, Y. H.; Wen, B.; Sachtler, W. M. H.; Weitz, E. *J. Phys. Chem. B* **2004**, *108*, 5386–5404.

(18) (a) Dathe, H.; Haider, P.; Jentys, A.; Lercher, J. A. *J. Phys. Chem. B* **2006**, *110*, 10729–10737. (b) Dathe, H.; Haider, P.; Jentys, A.; Lercher, J. A. *J. Phys. Chem. B* **2006**, *110*, 26024–26032.

(19) (a) Muneda, N.; Shibata, M.; Demura, M.; Kandori, H. *J. Am. Chem. Soc.* **2006**, *128*, 6294–6295. (b) Sato, Y.; Iwata, T.; Tokutomi, S.; Kandori, H. *J. Am. Chem. Soc.* **2005**, *127*, 1088–1089.

(20) Blanchet, L.; Ruckebusch, C.; Mezzetti, A.; Huvenne, J. P.; de Juan, A. *J. Phys. Chem. B* **2009**, *113*, 6031–6040.

(21) Tarantola, A. *Inverse Problem Theory: and Methods for Model Parameter Estimation*; SIAM: Philadelphia, PA, 2004.

(22) Engl, H. W.; Hanke, M.; Neubauer, A. *Regularization of Inverse Problems*; Kluwer Academic Publishers: Boston, 1996.

(23) Kügler, P.; Gaubitzer, E.; Müller, S. *J. Phys. Chem. A* **2008**, *113*, 2775–2785.

(24) Hadamard, J. *Sur les problèmes aux dérivées partielles et leur signification physique*, Princeton University Bulletin, 1902; pp 49−52.

(25) Vajda, S.; Rabitz, H. *J. Phys. Chem.* **1988**, *92*, 701–707.

(26) Vajda, S.; Rabitz, H.; Walter, E.; Lecourtier, Y. *Chem. Eng. Commun.* **1989**, *83*, 191–219.

(27) Shenvi, N.; Geremia, J. M.; Rabitz, H. *J. Phys. Chem. A* **2002**, *106*, 12315–12323.

(28) Neumaier, A. *SIAM Rev.* **1998**, *40*, 636–666.

(29) Kelley, C. T. *Iterative Methods for Optimization*; SIAM Frontiers in Applied Mathematics: Philadelphia, PA, 1999; No. 18.

(30) (a) Hansen, P. C. *Rank-Deficient and Discrete Ill-Posed Problems*; SIAM: Philadelphia, PA, 1998. (b) Golub, G. H.; Van Loan, C. F. *Matrix Computations*, 2nd ed.; John Hopkins University Press: Baltimore, MD, 1990; Chapter 8. (c) Press, W. H.; Teukolsky, S. A.; Vetterling, W. T.; Flannery, B. P. Numerical Recipes in C. In *The Art of Scientific Computing*, 2nd ed.; Cambridge University Press: New York, 1992.

(31) Chu, M. T. *SIAM Rev.* **1998**, *40*, 1–39.

(32) Dittmar, K; Siesler, W. H. *Fresenius' J. Anal. Chem.* **1998**, *362*, 109–113.

(33) Friebe, A.; Siesler, H. W. *Vib. Spectrosc.* **2007**, *43*, 217–220.

(34) (a) Jouquet, J. C. E. *J. Math. Pure Appl.* **1905**, *1*, 347–425. (b) Jouquet, J. C. E. *J. Math. Pure Appl.* **1906**, *2*, 5–85.(c) Jouquet, J. C. E. Mechanics of Explosives, Doin, 1917. In *Fundamental Bases of Chemical Thermodynamics*; Dode, Ed.; Sedes: Paris, 1956. (d) de Donder, T. In *Leçons de Thermodynamique et de Chimie Physique*; Van der Dungen, F. H., Van Lergerghe, G., Eds.; Gauthier-Villars: Paris, 1920. (e) Prigogine, I., Defay, R. *Chemical Thermodynamics*; Longmans Green: London−New York−Toronto, 1954.

(35) Dumon, A.; Lichanot, A.; Poquet, E. *J. Chem. Educ.* **1993**, *70*, 29–30.
(36) Steinfeld, J. I.; Francisco, J. S.; Hase, W. L. *Chemical Kinetics and Dynamics*; Prentice Hall: Englewood Cliffs, NJ, 1989.
(37) Jiang, J.-H.; Šašić, S.; Yu, R.-Q.; Ozaki, Y. *J. Chemom.* **2003**, *17*, 186–197.
(38) (a) Amrhein, M.; Srinivasan, B.; Bonvin, D.; Schumacher, M. M. *Chemom. Intell. Lab. Syst.* **1996**, *33*, 17–33. (b) Bhatt, N.; Amrhein, M.; Bonvin, D. *Ind. Eng. Chem. Res.* **2010**, *49*, 7704–7717.
(39) (a) Bernard, O.; Bastin, G. *Math. Biosci.* **2005**, *193*, 51–77. (b) Bernard, O.; Bastin, G. *Bioprocess. Biosyst. Eng.* **2005**, *27*, 293–301.
(40) Hulhoven, X.; Vande Wouwer, A.; Bogaerts, Ph. *Bioprocess. Biosyst. Eng.* **2005**, *27*, 283–291.
(41) Connors, K. A. *Chemical Kinetics: The Study of Reaction Rates in Solution*; VCH Publisher: New York, 1990; Chapter 3.
(42) Feinberg, M. *Chem. Eng. Sci.* **1988**, *43*, 1–25.
(43) Li, H.-Y.; Ho, P.-Y. *Ind. Eng. Chem. Res.* **2000**, *39*, 3291–3297.
(44) (a) Yin, F. *Ind. Eng. Chem. Res.* **1990**, *29*, 34–39. (b) Widjaja, E.; Li, C.; Garland, M. *J. Catal.* **2004**, *223*, 278–289. (c) Rajal, V. B.; Cuevas, C. M. *World J. Microbiol. Biotechnol.* **2008**, *24*, 1081–1090.
(45) (a) Kirkpatrick, S.; Gelatt, C. D.; Vecchi, M. P. *Science* **1983**, *220*, 671–680. (b) Corana, A.; Marchesi, M.; Martini, C.; Ridella, S. *ACM Trans. Math. Softw.* **1987**, *13*, 262–280.
(46) (a) Paatero, P.; Tupper, U. *Envirometrics* **1994**, *5*, 111–126. (b) Lee, D. D.; Seung, S. *Nature* **1999**, *401*, 788–791.
(47) Metropolis, N.; Rosenbluth, A.; Teller, A.; Teller, E. *J. Chem. Phys.* **1953**, *21*, 1087–1090.
(48) (a) Bonvin, D.; Rippin, D. W. T. *Chem. Eng. Sci.* **1990**, *45*, 3417–3426. (b) Amrhein, M.; Srinivasan, B.; Bonvin, D. *Chem. Eng. Sci.* **1999**, *54*, 579–591.
(49) Malinowski, E. R. *Factor Analysis in Chemistry*; Wiley: New York, 2002.
(50) (a) Amrhein, M. Reaction and Flow Variants/Invariants for the Analysis of Chemical Reaction Data. Doctoral Thesis 1861, EPFL: Switzerland, Lausanne, 1998. (b) Brendel, M.; Bonvin, D.; Marquardt, W. *Chem. Eng. Sci.* **2006**, *61*, 5404–5420.
(51) (a) Lórenz-Fonfría, V.; Kandori, H. *J. Am. Chem. Soc.* **2009**, *131*, 5891–5901. (b) Russi, T.; Packard, A.; Feeley, R.; Frenklach, M. *J. Phys. Chem. A* **2008**, *112*, 2579–2588.
(52) (a) Maeder, M.; Neuhold, Y.-M. In *Data Handling in Science and Technology: Practical Data Analysis in Chemistry*; Rutan, S., Walczak, B., Eds.; Elsevier: Amsterdam, 2007; Vol. 26. (b) Blobel, J.; Bernadó, P; Svergun, D.; Tauler, R.; Pons, M. *J. Am. Chem. Soc.* **2009**, *131*, 4378–4386.
(53) (a) Aris, R.; Mah, R. H. S. *Ind. Eng. Chem. Fundam.* **1963**, *2*, 90–94.(b) Aris, R. *Introduction to the Analysis of Chemical Reactor*; Prentice-Hall: Englewood Cliffs, NJ, 1965. (c) Yablonskii, G.; Bykov, V.; Gorban, A.; Elokhin, V. In *Comprehensive Chemical Kinetics: Kinetic Models of Catalytic Reactions*; Compton, R. G., Ed.; Elsevier: Amsterdam, 1991; Vol. 32.
(54) (a) Feinberg, M. *Chem. Eng. Sci.* **1987**, *42*, 2229–2268. (b) Feinberg, M. *Arch. Rational Mech. Anal.* **1995**, *132*, 371–406.